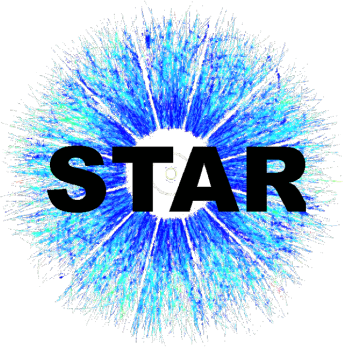

Production of Light Nuclei in Au+Au Collisions with the STAR BES-II Program

Yixuan Jin（金宜萱）

Central China Normal University

October 12, 2024

Outline

- Motivation
- The STAR Experiment
  - Dataset and Particle Identification
- Results in BES-I, FXT and Isobar
- Results in BES-II
  - Transverse Momentum Spectra
  - Particle Yields and Ratios
  - Coalescence Parameters
  - Nuclear Modification Factors
- Summary and Outlook

Motivation – QCD Phase Diagram and HIC

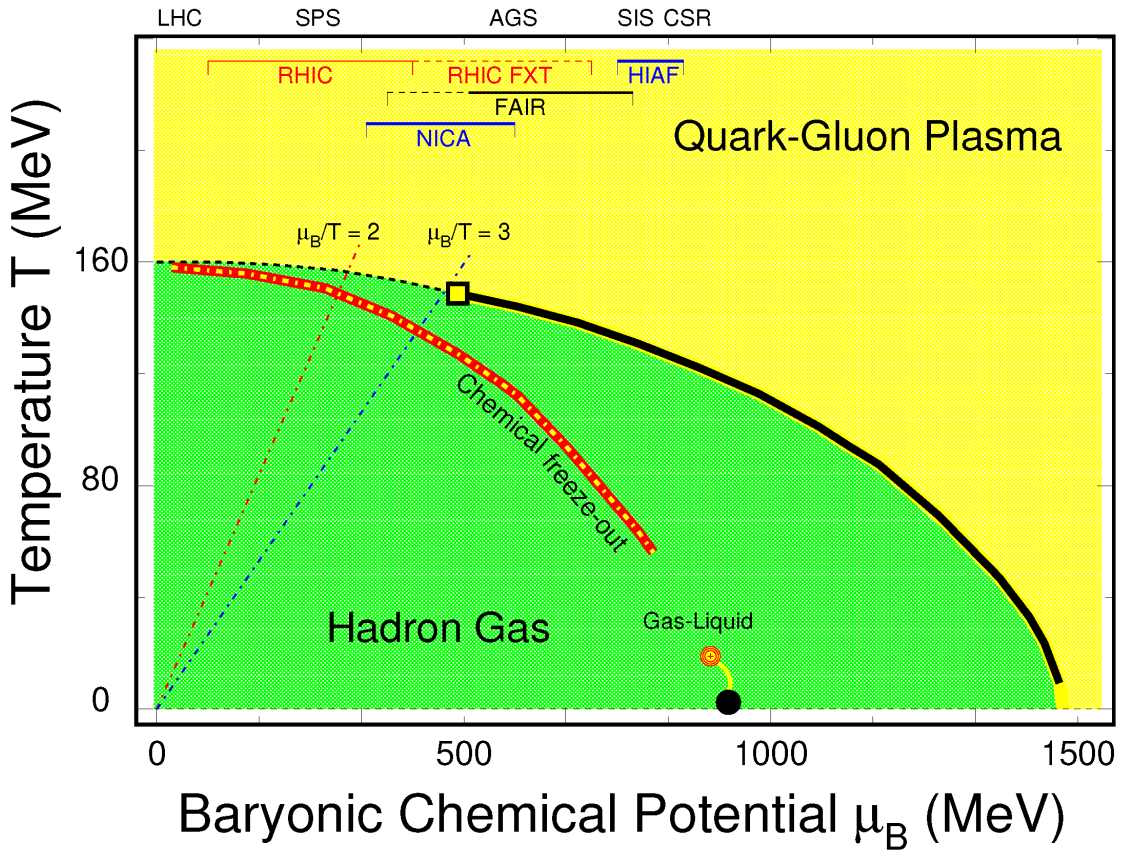

Beam Energy Scan Program at RHIC:

- Control beam energy and centrality to vary initial T and μ_B.
- Create QGP and explore its properties.
- Map out the crossover and/or 1st order QCD phase boundary.
- Search for the signatures of possible QCD critical point.

A. Bzdak, S. Esumi, V. Koch, J. F. Liao, M. Stephanov, and N. Xu. Physics Reports, 853 (2020) 1–87.
X. Luo, N. Xu, Nucl. Sci. Tech. 28, (2017) 112
X. Luo, Q. Wang, N. Xu, P. F. Zhuang. *Properties of QCD Matter at High Baryon Density.* Springer, 2022.
https://drupal.star.bnl.gov/STAR/starnotes/public/sn0598

Motivation – Light Nuclei

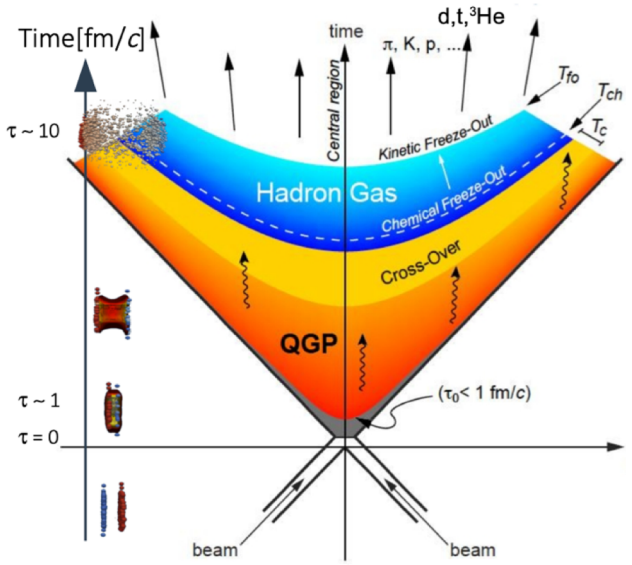

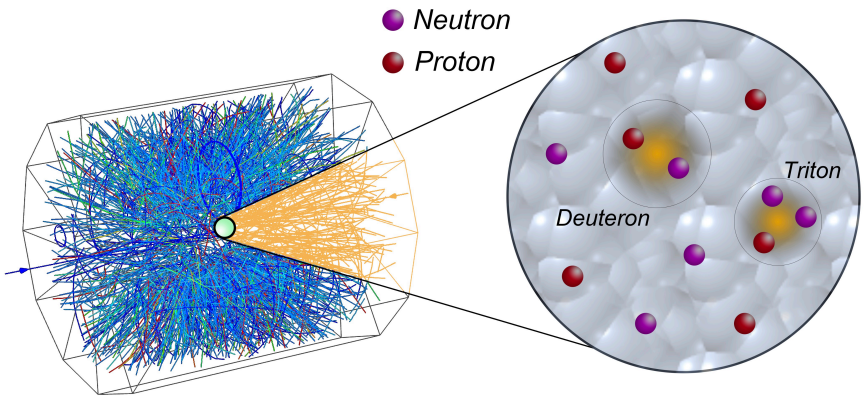

1. Why Light Nuclei?

- May carry information about local baryon density fluctuations.
- Provide an effective probe to study 1st order phase boundary and the QCD critical point.

2. Observable : Yield ratio of light nuclei $(N_t \times N_p / N_d^2)$

- Based on coalescence model:

$$N_A = g_c \int d\Gamma \rho_s(\{x_i, p_i\}) \times W_A(\{x_i, p_i\})$$

- The yield ratio is related to neutron density fluctuations:

$$N_t \times N_p / N_d^2 \approx g(1 + \Delta n)$$

factor $g = \frac{1}{2\sqrt{3}}$ comes from the thermal equilibrium assumption of nucleon abundances.

K. Sun et al. Phys.Lett.B 774 (2017) 103-107
E. Shuryak et al. Phys.Rev.C 101 (2020) 3, 034914

RHIC Beam Energy Scan Program

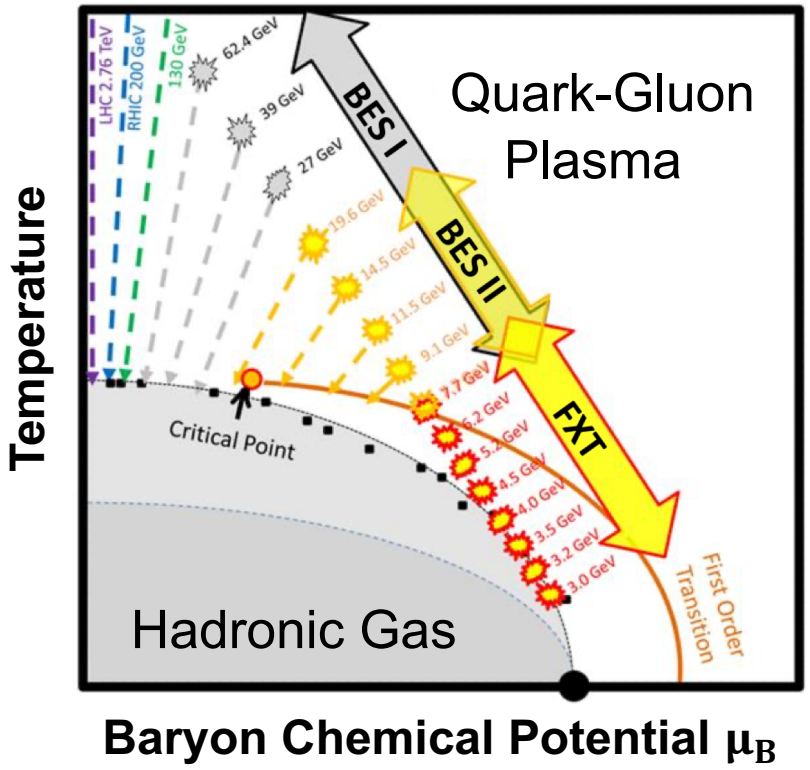

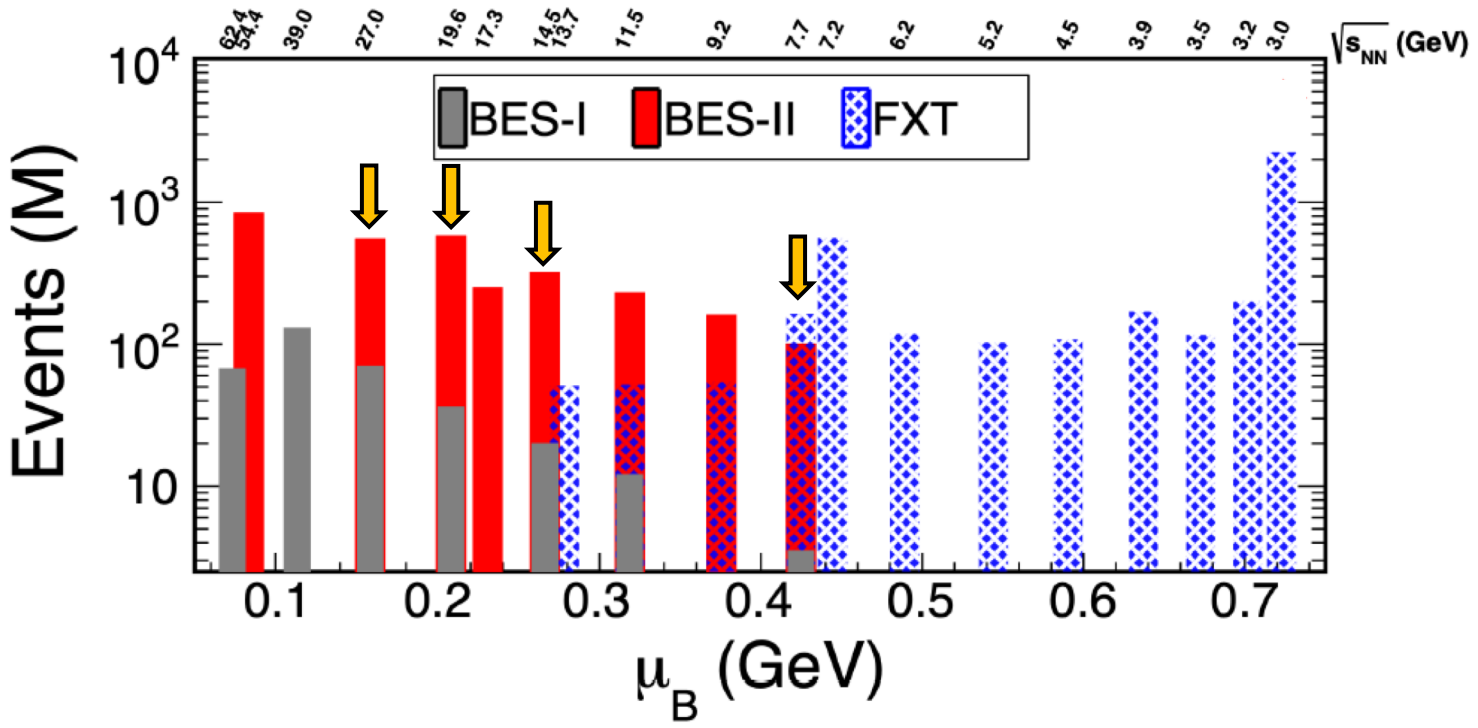

- STAR has completed BES-II data-taking with factors of 10 – 20 more statistics compared to BES-I.
- BES-II: 8 collider energies ($\sqrt{s_{\mathrm{NN}}}$ = 7.7 – 54 GeV) / 12 FXT energies ($\sqrt{s_{\mathrm{NN}}}$ = 3.0 – 13.7 GeV)
- μ_{B} coverage : 25 < μ_{B} < 750 MeV.

STAR Collaboration, arXiv:1007.2613
https://drupal.star.bnl.gov/STAR/starnotes/public/sn0493
https://drupal.star.bnl.gov/STAR/starnotes/public/sn0598

The Solenoidal Tracker At RHIC (STAR)

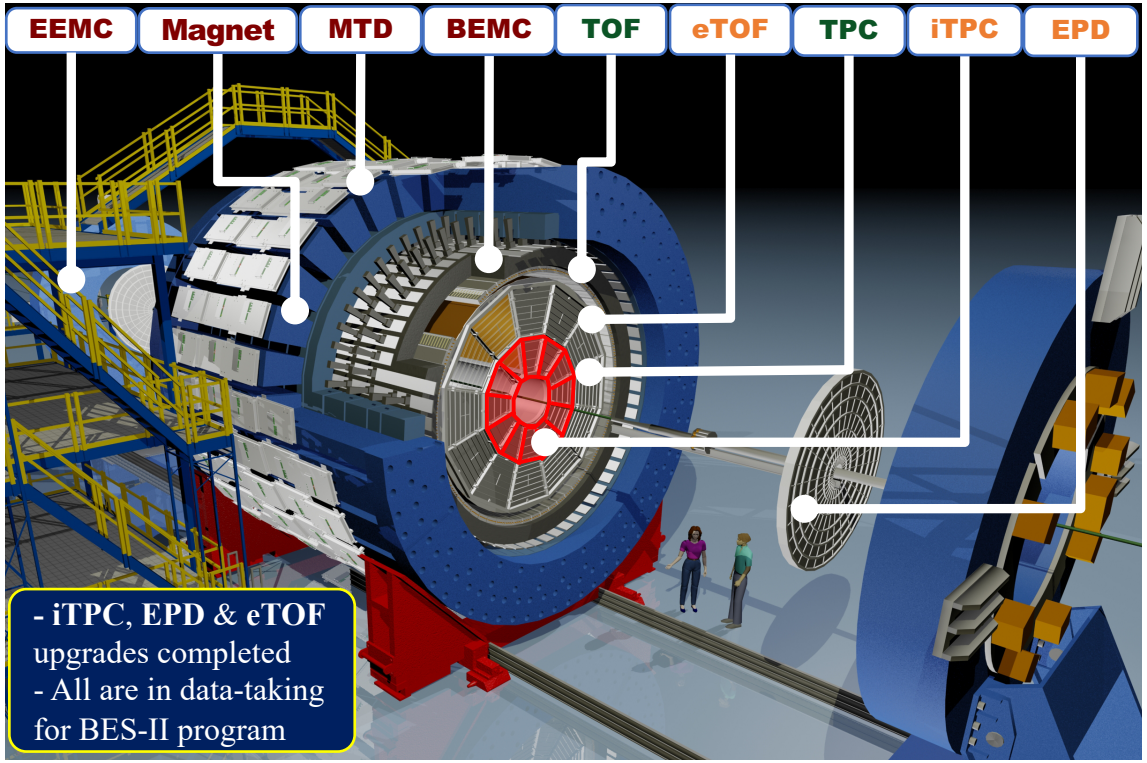

Detector upgrades for STAR BES-II

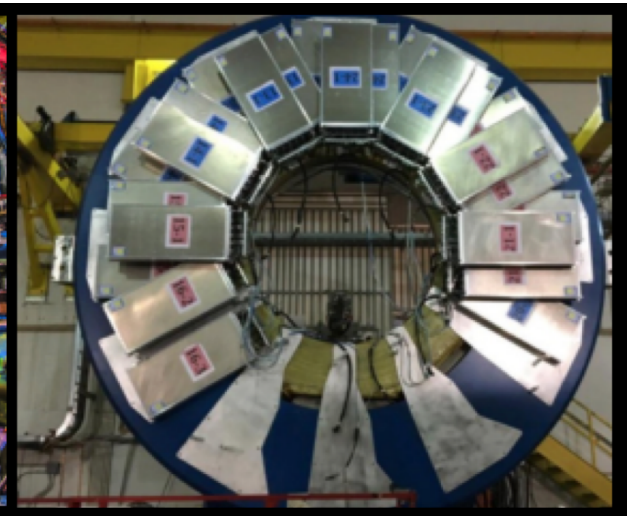

iTPC:
- Improves $\mathrm{d}E/\mathrm{d}x$
- Extends η coverage from 1.0 to 1.5
- Lower p_{T} cut-in from 125 to 60 MeV/c
- Ready in 2019

eTOF:
- Forward rapidity coverage
- η coverage from 1.0 to 1.5
- Borrowed from CBM-FAIR
- Ready in 2019

iTPC: https://drupal.star.bnl.gov/STAR/starnotes/public/sn0619
eTOF: STAR and CBM eTOF group, arXiv: 1609.05102

- **Enlarge the rapidity acceptance**
- **Improve particle identification**
- **Lower p_{T} cut-in to reduce uncertainty in spectra extrapolation**

Results from RHIC BES-I

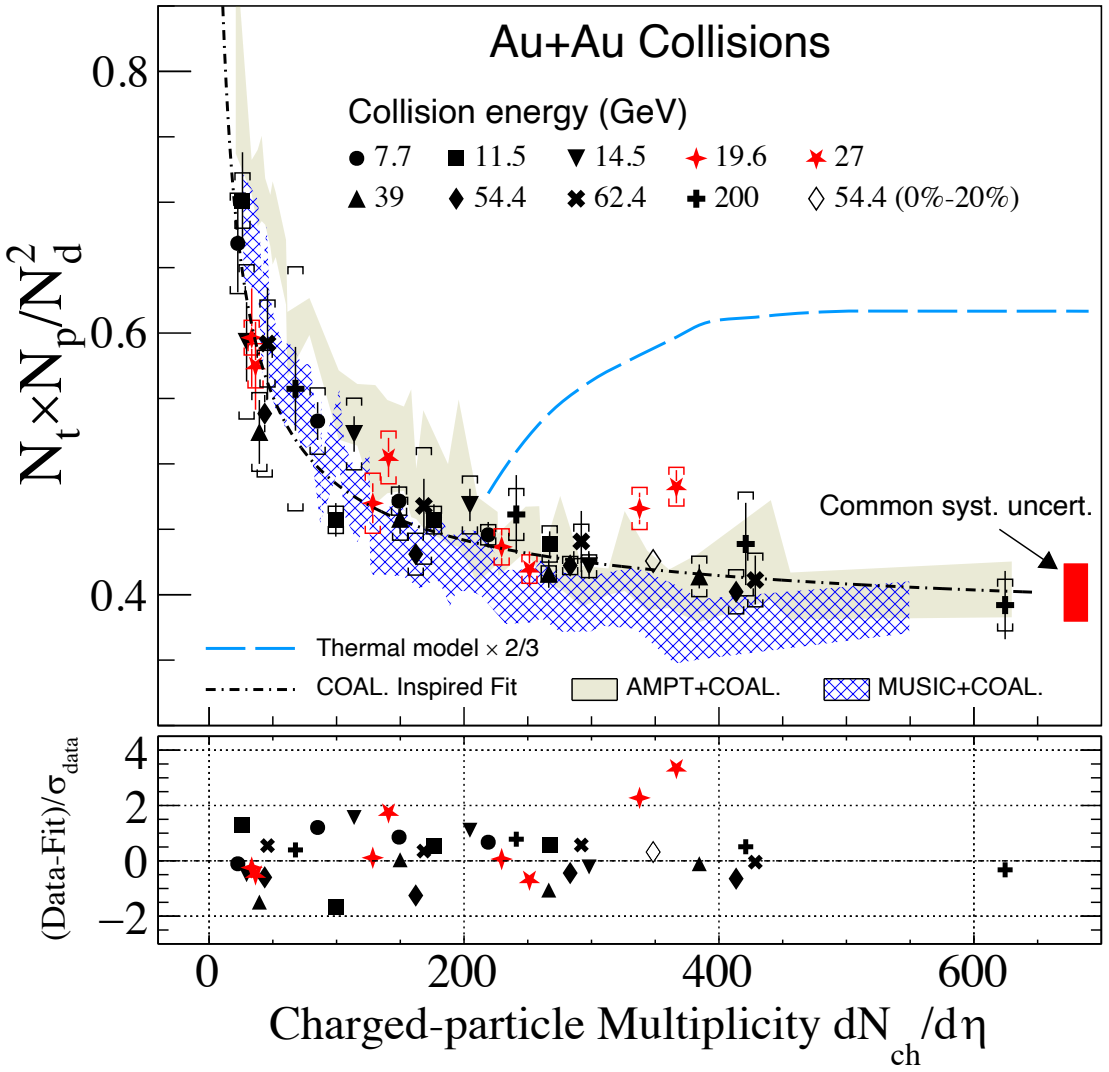

STAR Collaboration, Phys.Rev.Lett. 130 (2023) 202301

- The yield ratio exhibits a scaling behavior: A trend driven by the interplay between the size of light nuclei and the size of the fireball created in HIC.

$$\frac{N_t \times N_p}{N_d^2} = p_0 \times \left(\frac{R^2 + \frac{2}{3} r_d^2}{R^2 + \frac{1}{2} r_t^2} \right)^3 , \text{where } R \propto (dN_{ch}/d\eta)^{1/3}.$$

W. Zhao, K. J. Sun, C. M. Ko and X. Luo, Phys. Lett. B 820 (2021) 136571

- The ratios at $\sqrt{s_{NN}}$ = 19.6 and 27 GeV in 0-10% centrality show enhancements with respect to the coalescence baseline with a combined significance of 4.1σ.

- The thermal model overestimates the experimental data and shows a clear difference compared to the coalescence model.

Results from RHIC FXT at $\sqrt{s_{NN}}$ = 3 GeV

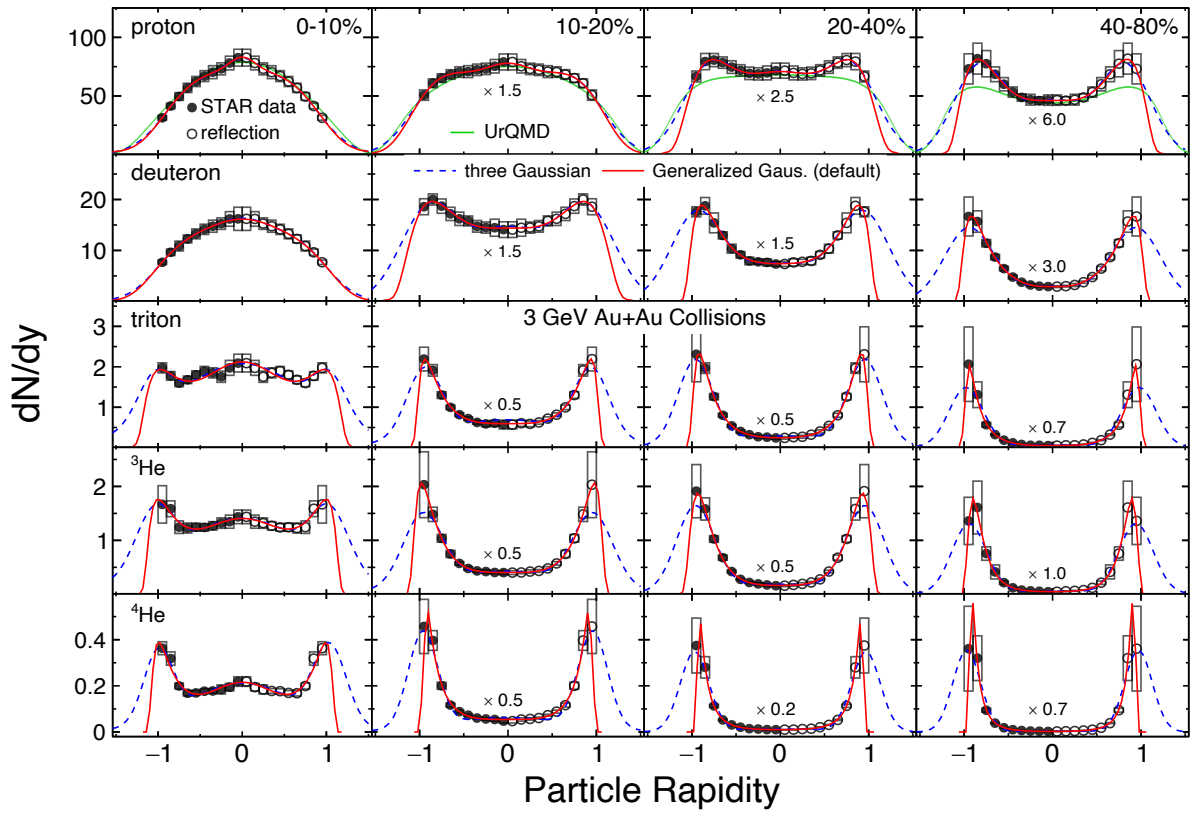

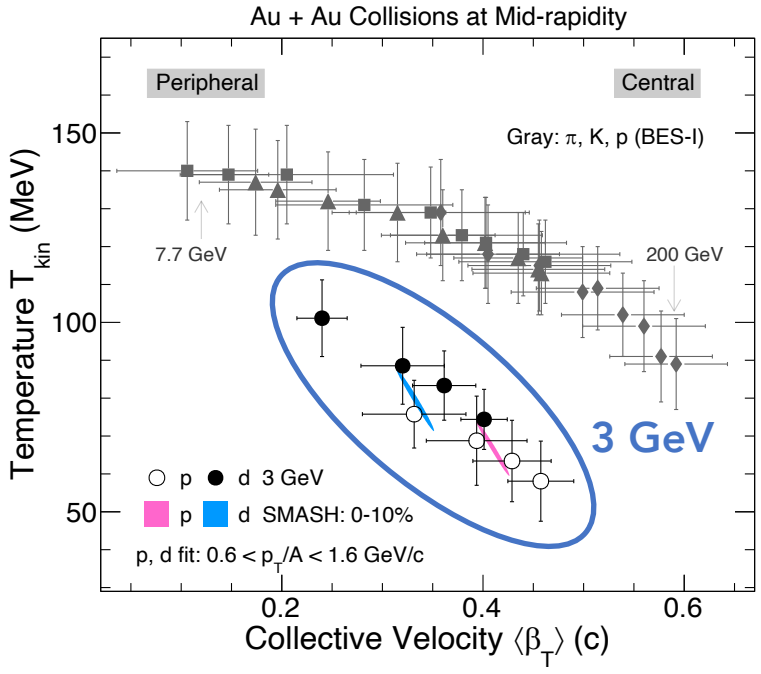

Blast-Wave: $\frac{1}{2\pi p_T}\frac{d^2N}{dp_T dy} \propto \int_0^R r dr m_T I_0\left(\frac{p_T \sinh\rho}{T_{kin}}\right) K_1\left(\frac{m_T \cosh\rho}{T_{kin}}\right)$

STAR Collaboration, arXiv: 2311.11020
K.J. Sun, W.H. Zhou, L.W. Chen, C.M. Ko, F. Li, R. Wang, J. Xu, arXiv: 2205.11010

- The centrality dependence of rapidity density is attributed to the interplay between baryon stopping and the spectators' contribution.
- At 3 GeV Au+Au collisions, the kinetic freeze-out parameters (T_{kin}, $\langle\beta_T\rangle$) show different trend compared to that of higher energy collisions.
- The freeze-out parameter (T_{kin}) of deuteron is systematically higher than that of proton at 3 GeV, which is different from higher energies.

→ Indicate a different equation of state (EoS)

Similar trend seen in SMASH Model
$T_{kin}^{d} > T_{kin}^{p}$

Results from RHIC Isobar

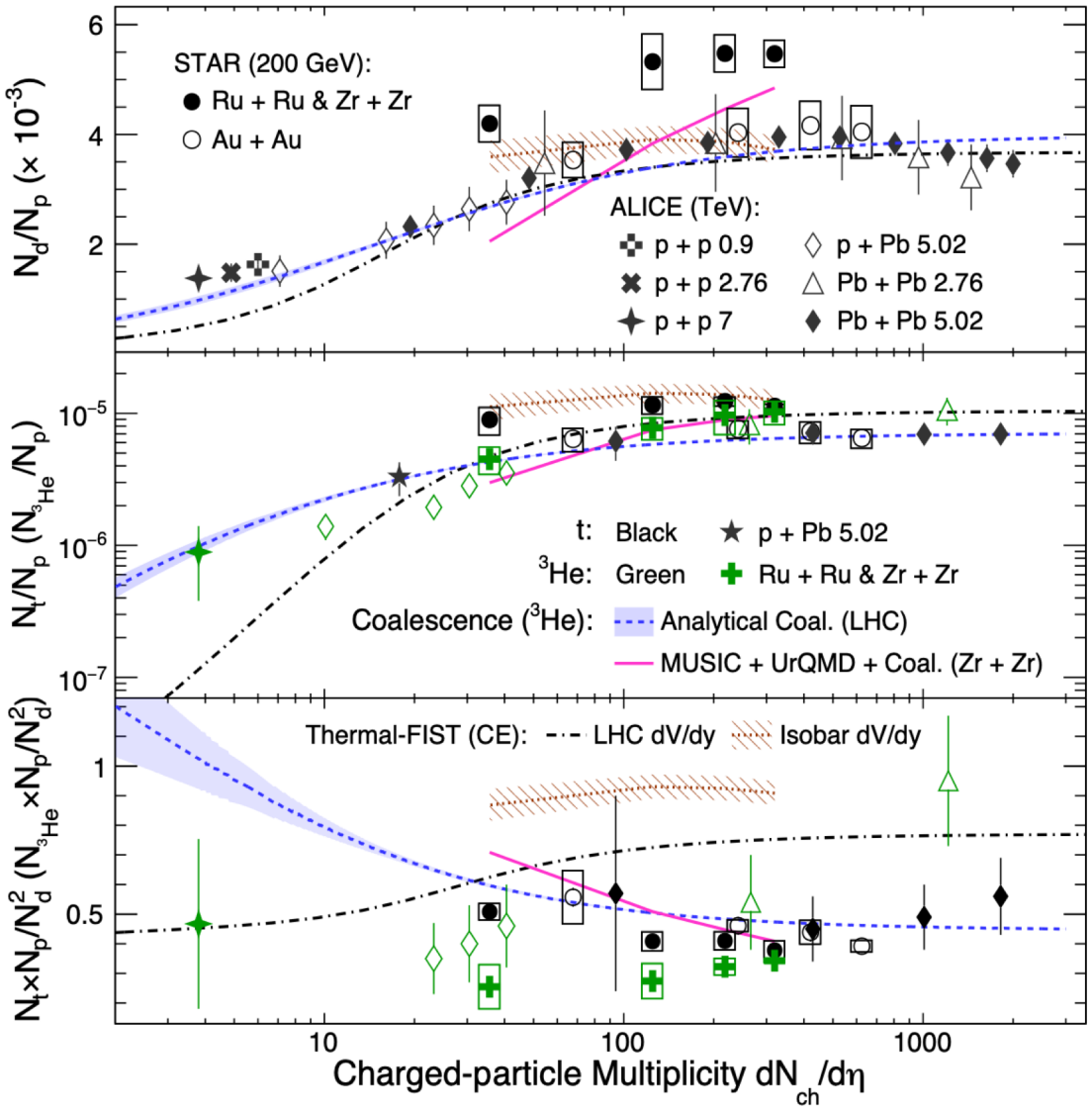

- Deuteron production are enhanced in Ru\Zr + Ru\Zr collisions compared with other systems.
- Triton yield deviate from $^3\mathrm{He}$ yield in peripheral collision which may effected by neutron skin.
- $N_\mathrm{t} \times N_\mathrm{p}/N_\mathrm{d}^2$ are overestimated by the thermal model.

V. Vovchenko, et al. Phys.Lett.B 785 (2018) 171-174
K-J. Sun, et al. Phys.Lett.B 792 (2019) 132-137; arXiv:2404.02701
[STAR Collaboration] Phys.Rev.C 99 (2019) 6, 064905; Phys.Rev.Lett. 130 (2023) 202301
[ALICE Collaboration] Phys.Rev.C 88 (2013) 044910; Phys.Rev.C 93 (2016) 2, 024917; Phys.Rev.C 107 (2023) 6, 064904

Particle Identification and Signal Extraction

TPC: $z = \log\left(\frac{\langle dE/dx \rangle_{measure}}{\langle dE/dx \rangle_{Bichsel}}\right)$

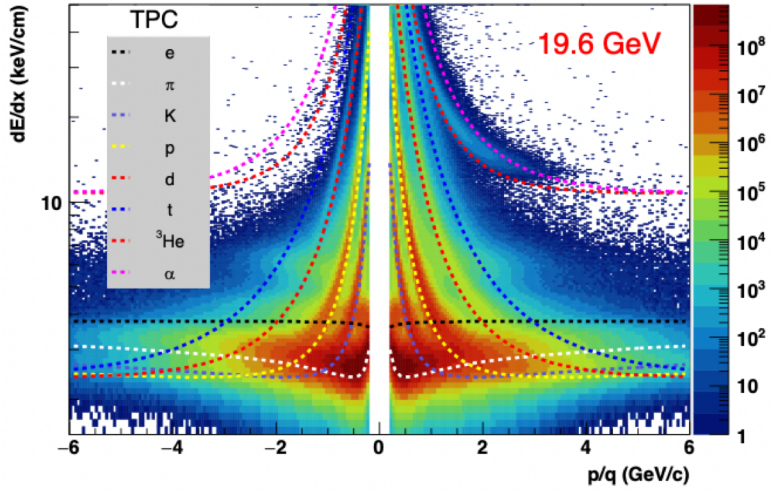

Signal Extraction Examples $(19.6\ \mathrm{GeV}, \mathrm{deuteron}, 0\text{-}5\%)$

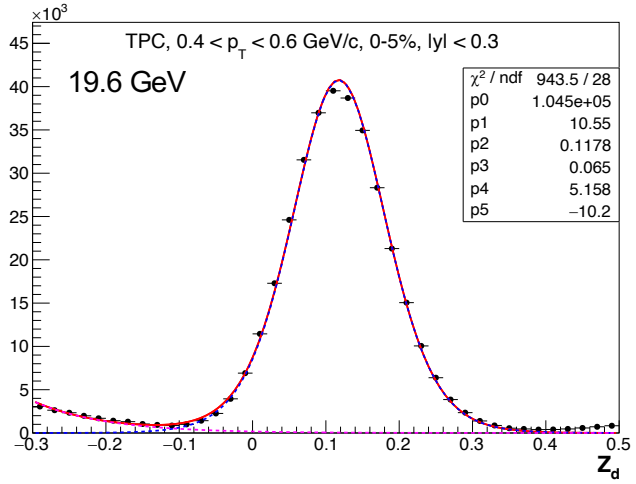

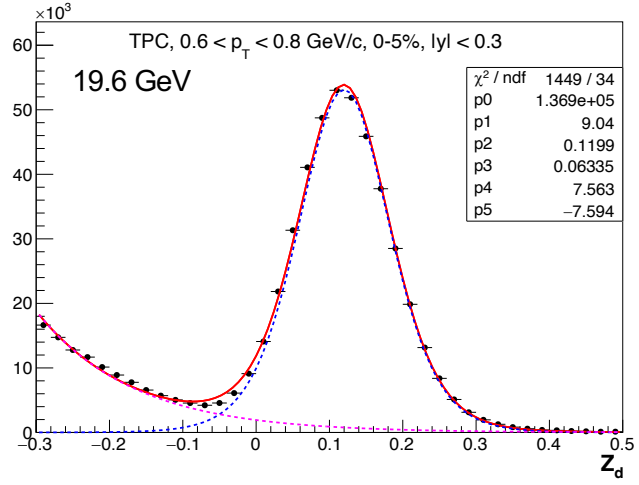

Low p_T: TPC

Signal: Gaussian (Blue)
BG: Gaussian (Magenta)
Total: (Red)

TOF: $\frac{m^2}{q^2} = \frac{p^2}{q^2}\left(\frac{c^2t^2}{L^2} - 1\right)$

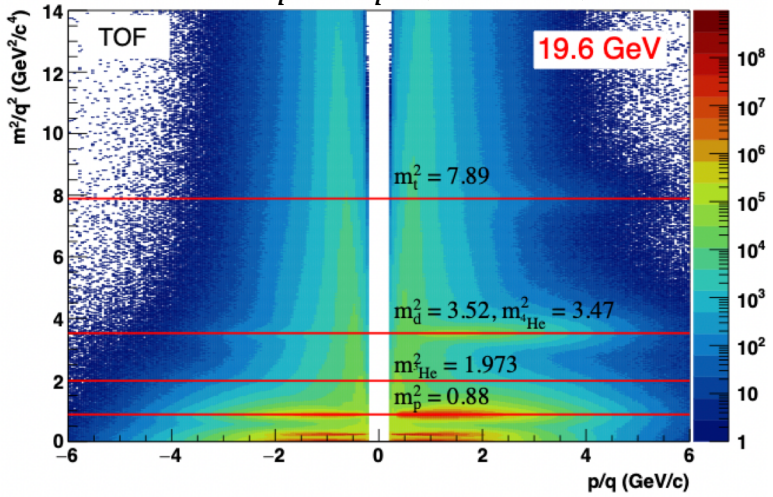

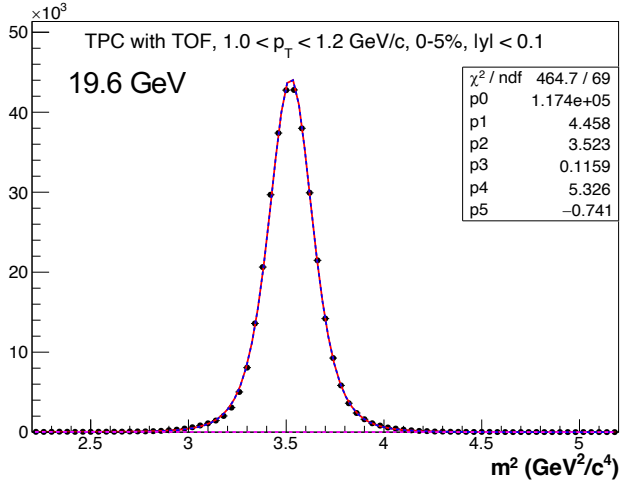

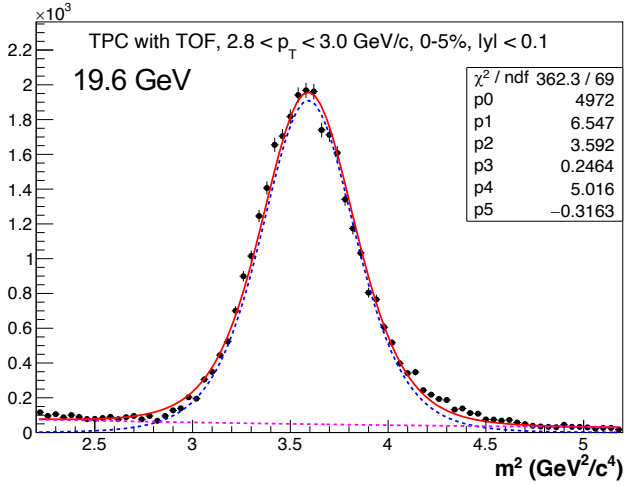

High p_T: TPC with TOF

Signal: Student-t (Blue)
BG: Gaussian (Magenta)
Total: (Red)

Transverse Momentum Spectra

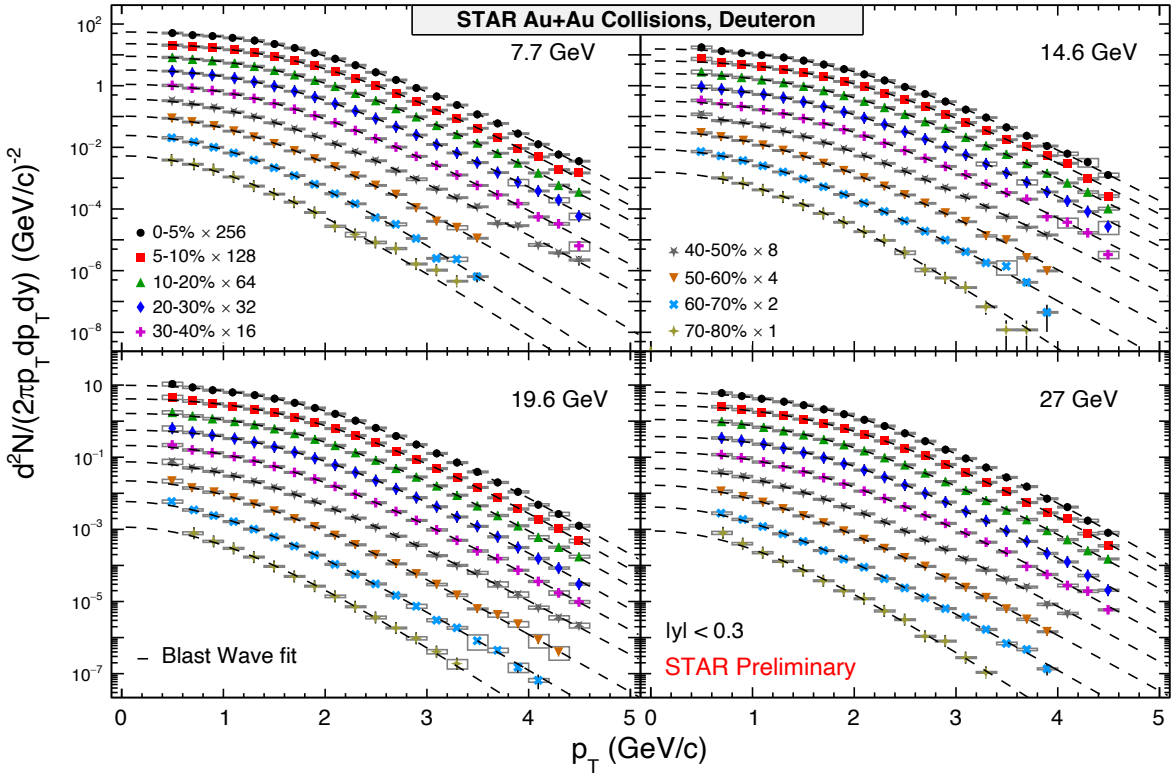

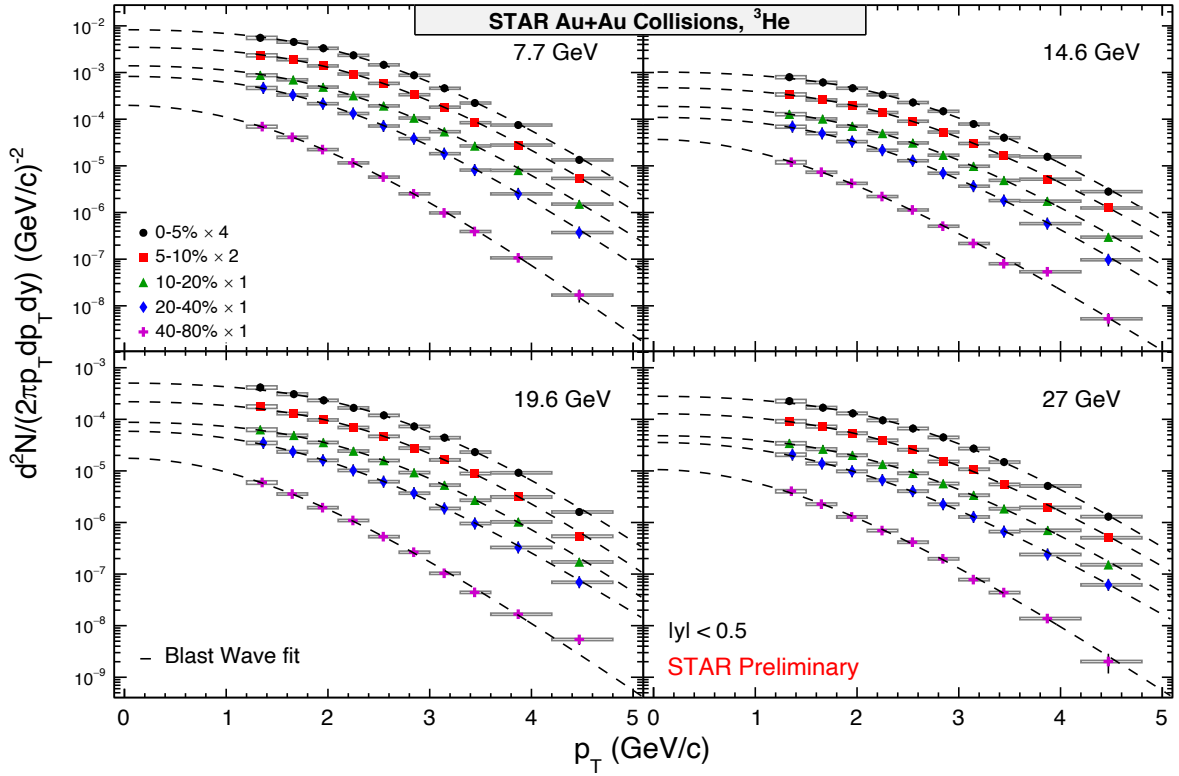

❖ Blast-Wave Function

$$\frac{1}{2\pi p_T}\frac{d^2N}{dp_T dy} \propto \int_0^R r dr m_T I_0\left(\frac{p_T \sinh\rho}{T_{kin}}\right) K_1\left(\frac{m_T \cosh\rho}{T_{kin}}\right)$$

$\rho = \tanh^{-1}\beta_r$, $\beta_r(r) = \beta_T\left(\frac{r}{R}\right)^n$, n fix to 1 in this analysis

Freeze-out parameters:

T_{kin} : kinetic freeze-out temperature

$\langle\beta_T\rangle$: average radial flow velocity

I_0 and K_1 : from Bjorken Hydrodynamic assumption

- All efficiencies and corrections are included.
- The statistical and systematic uncertainties are shown as vertical lines and boxes, respectively.
- The p_T ranges are extended in BES-II, which lead to smaller systematic uncertainties in particle yields.

(anti-)Proton Weak Decay Feed-down Correction

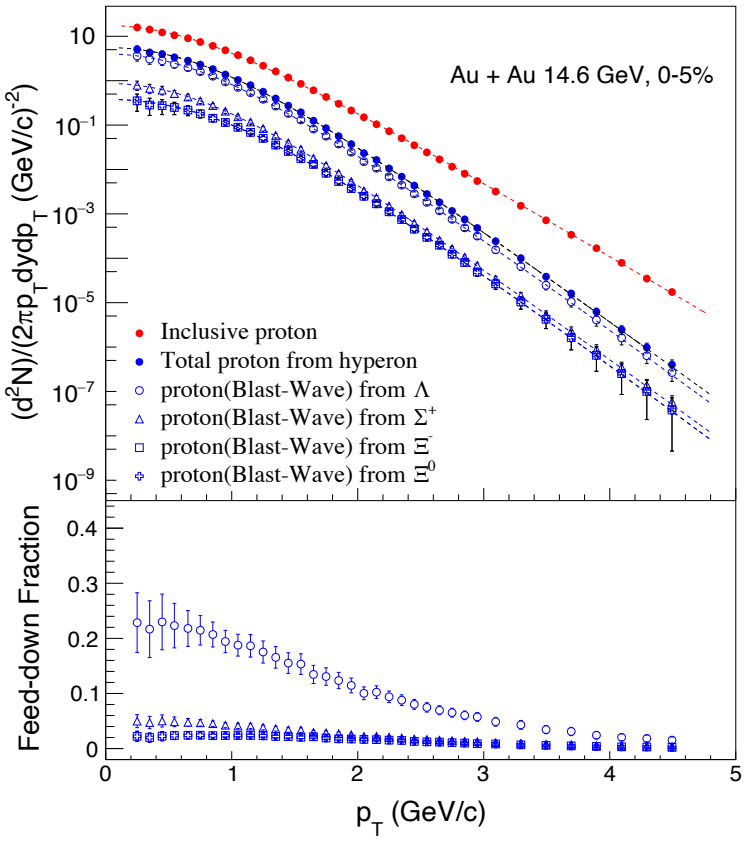

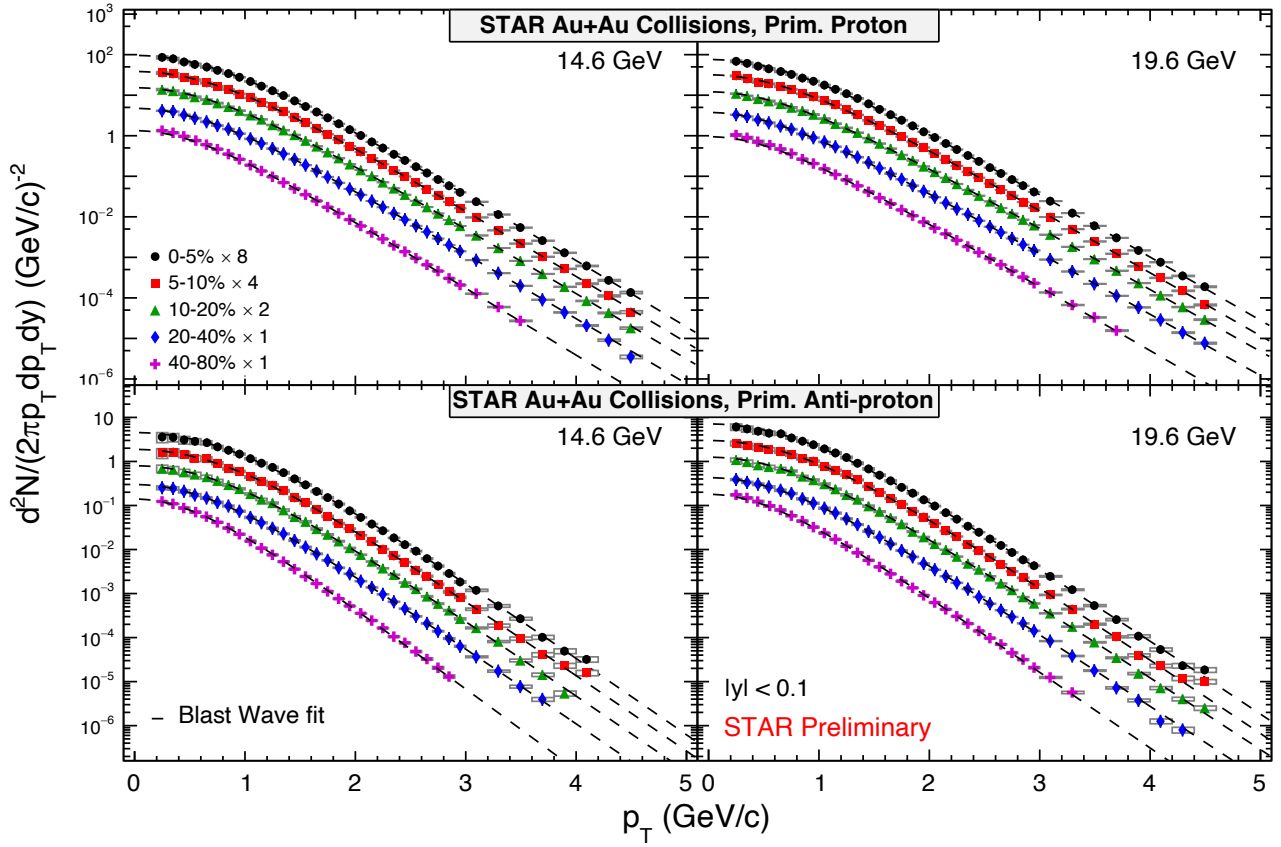

$\Lambda \rightarrow p + \pi^-$, branching ratio = 63.9 %
$\Sigma^+ \rightarrow p + \pi^0$, branching ratio = 51.57 %
$\Xi^- \rightarrow \Lambda + \pi^-$, branching ratio = 99.887 %
$\Xi^0 \rightarrow \Lambda + \pi^0$, branching ratio = 99.524 %

- The primordial spectra were obtained by subtracting the (anti-)proton weak decayed from strange hadrons.
- Data driven method: Use STAR published strange particle $(\Lambda, \Sigma^+, \Xi^-, \Xi^0)$ yields and embedding simulation samples.
- The spectra of Σ^+: Obtained by multiplying the Λ spectra by a factor of 0.27.
- The spectra of Ξ^0: Assumed to be the same as those of Ξ^-.

Particle Yields and Ratios

Inclusive Proton

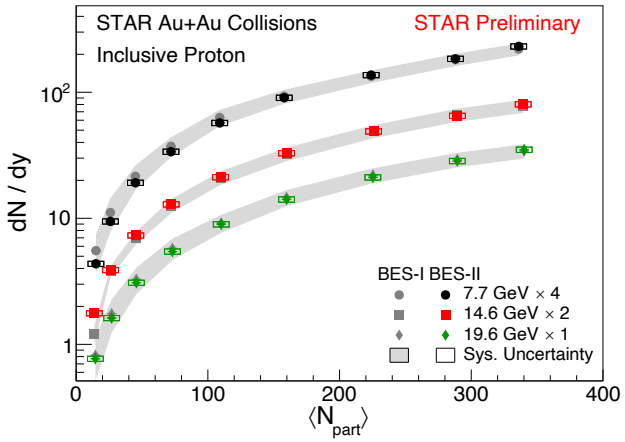

Primordial Proton

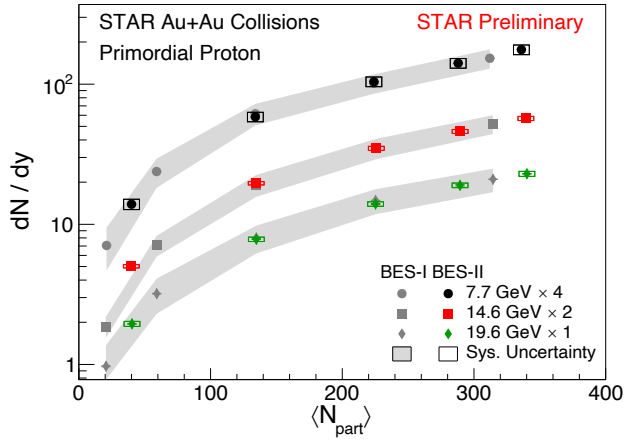

Deuteron

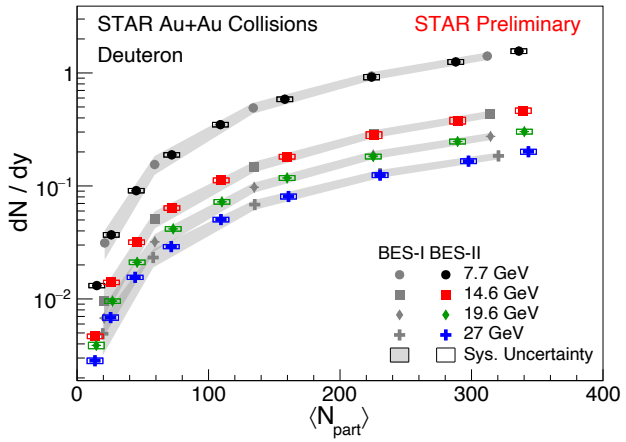

^{3}He

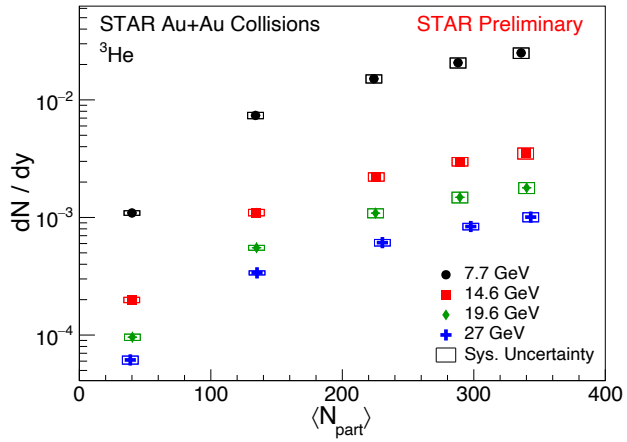

Inclusive Anti-proton

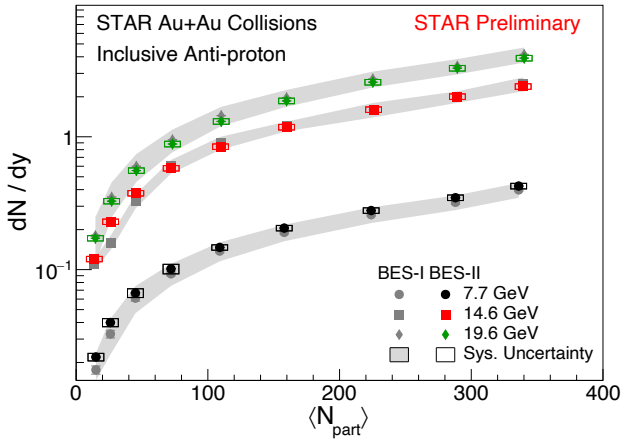

Primordial Anti-proton

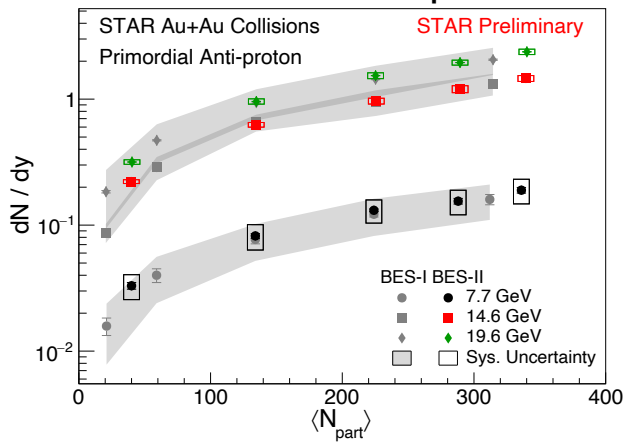

Anti-deuteron

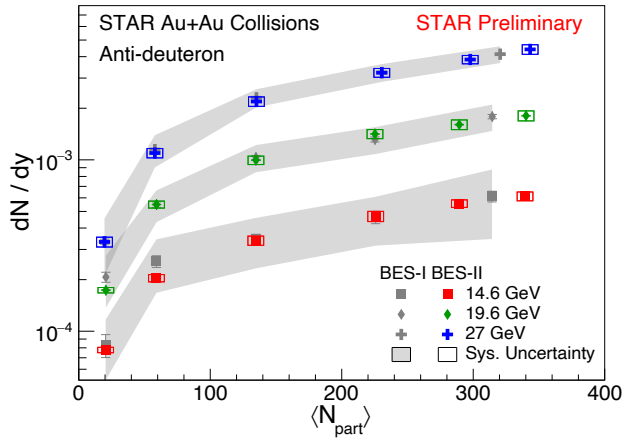

- The systematic uncertainties are reduced in BES-II because the p_T ranges are extended.
- Yields for light nuclei increase from peripheral to central collisions.
- dN/dy for positive particles decrease with increasing energy, while the behavior is opposite for antiparticles.

Particle Yields and Ratios

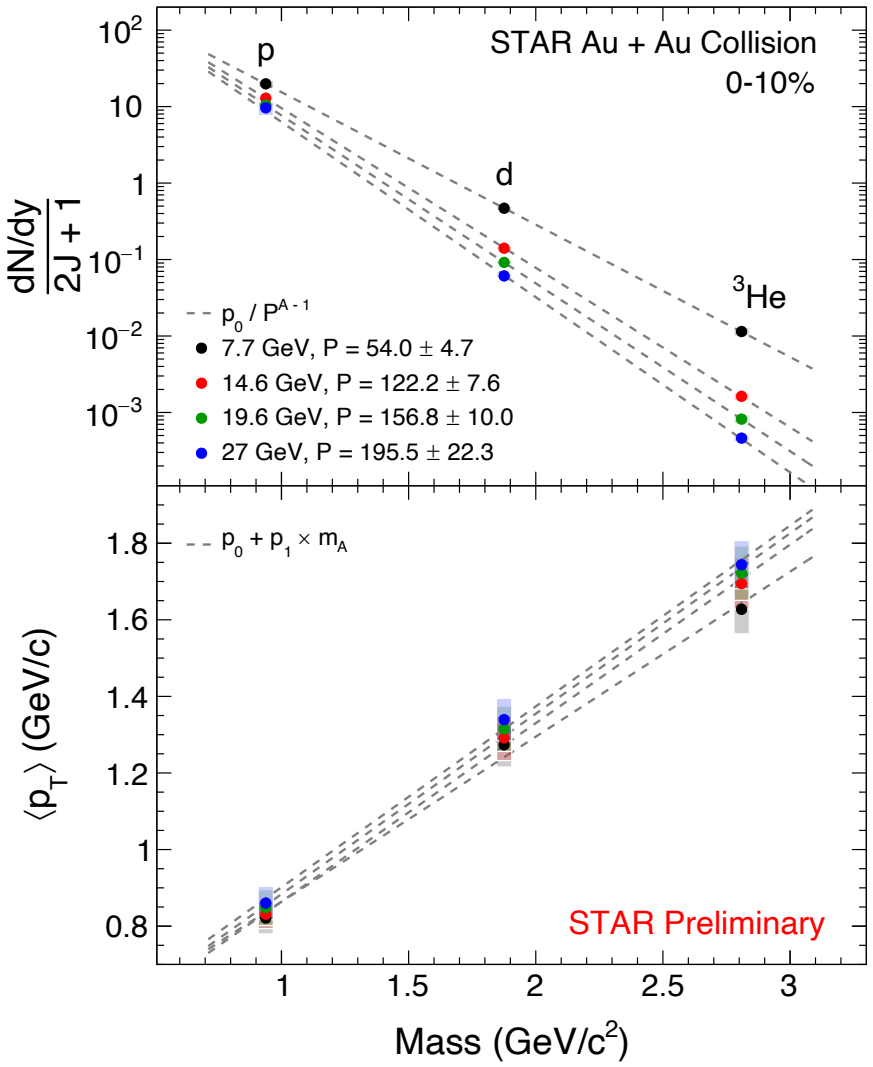

- Mass dependence of $\frac{dN/dy}{2J+1}$:
  - Fitted by an exponential function form p_0/P^{A-1},

    where P is the penalty factor and can be determined by the Boltzmann factor $e^{(m_N-\mu_B)/T}$ in thermal model.
  - The production of light nuclei are proportional to the spin degeneracy.
  - The penalty factor is larger at higher beam energy, which indicates that it is harder to form high-mass objects.

E864 Collaboration, Phys.Rev.Lett. 83 (1999) 5431-5434
STAR Collaboration, Phys.Rev.Lett. 130 (2023) 202301

- Mass dependence of $\langle p_T \rangle$:
  - Fitted by an linear function form $p_0 + p_1 \times m_A$.
  - The $\langle p_T \rangle$ increases linearly with increasing mass of the particles.

Particle Yields and Ratios

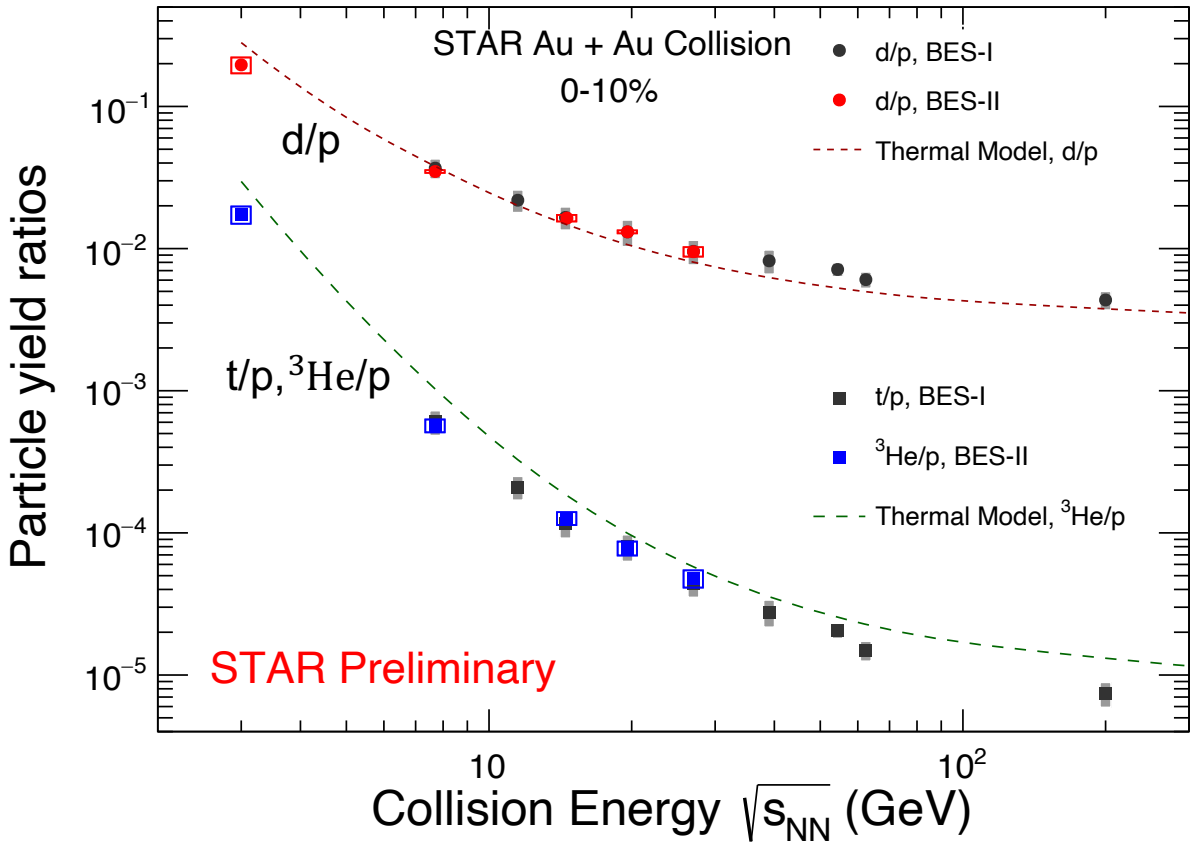

STAR, Phys. Rev. Lett. 130, 202301 (2023)

- The particle ratios are consistent with BES-I.
- The particle ratios show a monotonic decrease with collision energy.
- d/p ratio can be described well by the thermal model.
- The thermal model overestimates t/p and $^3He/p$ by a factor of approximately two.
  - The hadronic re-scatterings may play a crucial role during the hadronic expansion phase which lead to this discrepancy.

V. Vovchenko, B. Dönigus, B. Kardan, M. Lorenz, and H. Stoecker, Phys. Lett. B, (2020) 135746;

K.J. Sun, R. Wang, C. M. Ko, Y.G. Ma, and C. Shen, Nature Commun, 15 (2024) 1, 1074

Particle Yields and Ratios

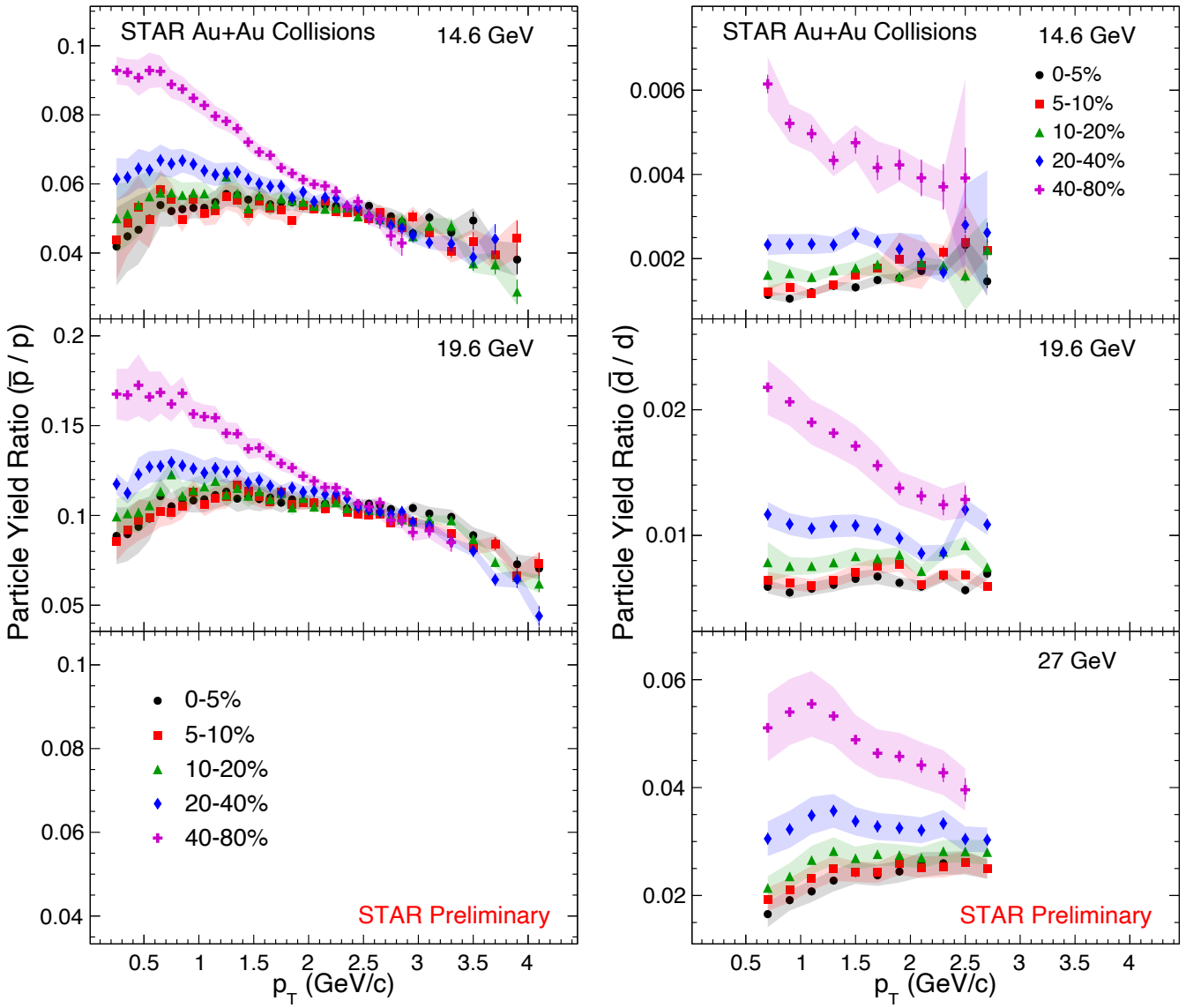

- The statistical and systematic uncertainties are shown as vertical lines and color bands, respectively.
- $\bar{p}/p$ and $\bar{d}/d$ ratios show strong centrality dependence.
  - This could be due to the annihilation between the particles and antiparticles.

Coalescence Parameter

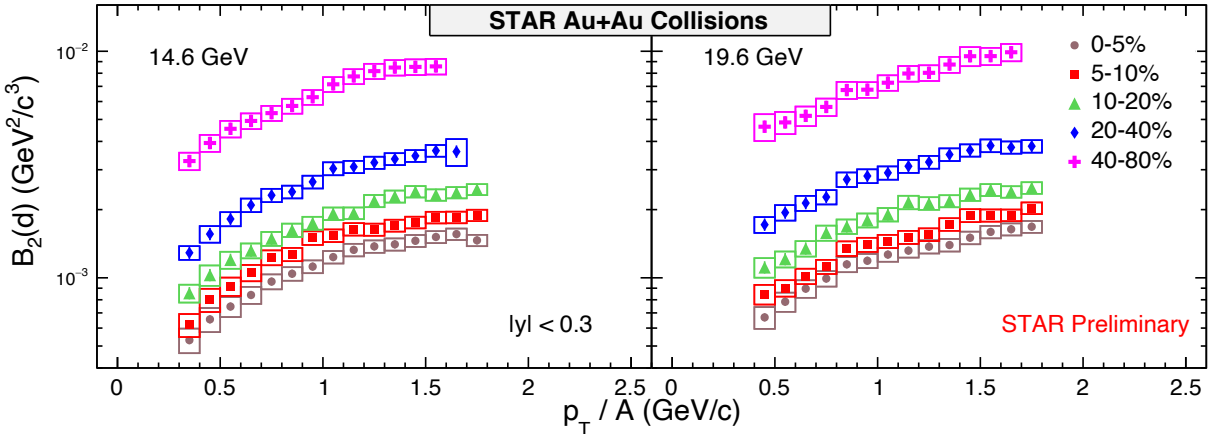

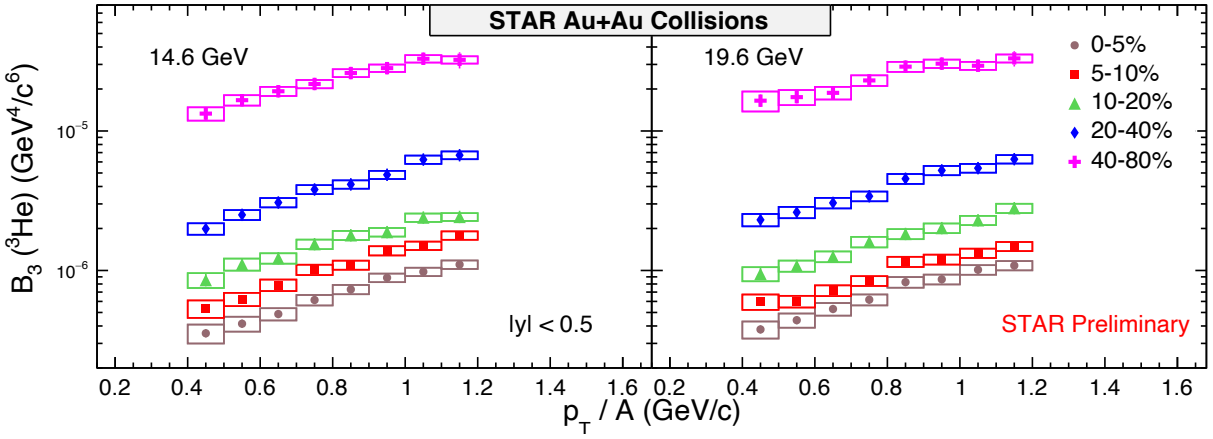

- In the coalescence picture, the invariant yield of light nuclei is proportional to the invariant yield of nucleons. The coalescence parameter B_{A} reflects the probability of nucleon coalescence, which is related to the local nucleon density.

$$E_{\mathrm{A}}\frac{\mathrm{d}^3N_{\mathrm{A}}}{\mathrm{d}^3p_{\mathrm{A}}} = B_{\mathrm{A}}\left(E_{\mathrm{p}}\frac{\mathrm{d}^3N_{\mathrm{p}}}{\mathrm{d}^3p_{\mathrm{p}}}\right)^{\mathrm{Z}}\left(E_{\mathrm{n}}\frac{\mathrm{d}^3N_{\mathrm{n}}}{\mathrm{d}^3p_{\mathrm{n}}}\right)^{\mathrm{A-Z}} \approx B_{\mathrm{A}}\left(E_{\mathrm{p}}\frac{\mathrm{d}^3N_{\mathrm{p}}}{\mathrm{d}^3p_{\mathrm{p}}}\right)^{\mathrm{A}}.$$

R. Scheibl and U. Heinz Phys.Rev.C 59 (1999) 1585-1602
STAR Collaboration, Phys.Rev.C 99 (2019) 6, 064905

- B_{A} increase with increasing p_{T} which might indicate an expanding collision system.
- B_{A} increase from central to peripheral collisions, which can be explained by a decreasing source volume.

Nuclear Modification Factors (R_{cp})

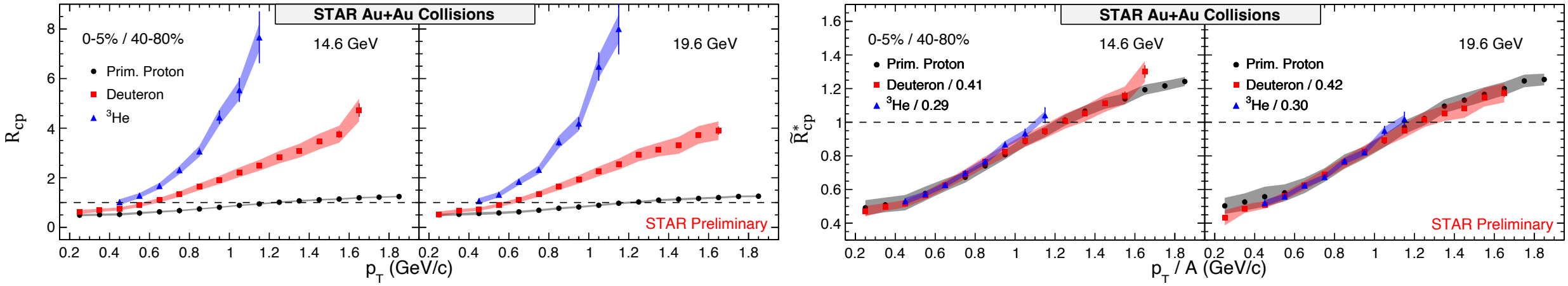

- $R_{\mathrm{cp}}(p_{\mathrm{T}}) = \frac{\langle N_{\mathrm{coll}}\rangle_{\mathrm{p}}}{\langle N_{\mathrm{coll}}\rangle_{\mathrm{c}}} \times \frac{\mathrm{d}^2 N_{\mathrm{AA}}^{\mathrm{c}}/\mathrm{d}p_{\mathrm{T}}\mathrm{d}y}{\mathrm{d}^2 N_{\mathrm{AA}}^{\mathrm{p}}/\mathrm{d}p_{\mathrm{T}}\mathrm{d}y}$, $\langle N_{\mathrm{coll}}\rangle$ is the average number of binary nucleon−nucleon collisions per event.
- Number of constituent nucleon (NCN) scaling for $R_{\mathrm{cp}}(p_{\mathrm{T}})$:

$$R_{\mathrm{cp}}^{*}(p_{\mathrm{T}}) = \left(\frac{B_{A,\,\mathrm{Central}}}{B_{A,\,\mathrm{Peripheral}}}\right)^{-1/A} \left(R_{\mathrm{cp}}(Ap_{\mathrm{T}})\right)^{1/A} \left(\frac{\langle N_{\mathrm{coll}}\rangle_{\mathrm{c}}}{\langle N_{\mathrm{coll}}\rangle_{\mathrm{p}}}\right)^{1/A-1} \equiv \left(\frac{B_{A,\,\mathrm{Central}}}{B_{A,\,\mathrm{Peripheral}}}\right)^{-1/A} \tilde{R}_{\mathrm{cp}}^{*}(p_{\mathrm{T}})$$

C. S. Zhou, Y. G. Ma, and S. Zhang. Eur.Phys.J.A 52 (2016) 12, 354

- R_{cp} for different particles exhibit distinct trends at all energies.
- In coalescence picture, the $\tilde{R}_{\mathrm{cp}}^{*}$ of light nuclei will follow a common trend when scaled by a constant factor, which is determined by $\tilde{R}_{\mathrm{cp}}^{*\ \mathrm{Nuclei}}/\tilde{R}_{\mathrm{cp}}^{*\ \mathrm{Proton}}$ at p_{T}/A = 0.65 GeV/c.

Summary and Outlook

Summary:

- We report the light nuclei productions (p, d, $^{3}\mathrm{He}$, $\bar{\mathrm{p}}$ and $\bar{\mathrm{d}}$) in Au+Au collisions at $\sqrt{s_{\mathrm{NN}}} = 7.7 - 27$ GeV from RHIC STAR BES-II.
- The particle ratios $N_{\mathrm{d}}/N_{\mathrm{p}}$ and $N_{^{3}\mathrm{He}}/N_{\mathrm{p}}$ have been measured.
  - The particle ratios show a monotonic decrease with collision energy.
  - The thermal model over-predicts t/p and $^{3}\mathrm{He}$/p by a factor of about 2.
- The coalescence parameter B_{A} have been measured.
  - Collective expansion leads to an increase in B_{A} from low to high p_{T}
  - Decreasing source volume results in a rise of B_{A} from central to peripheral collisions.
- The nuclear modification factor R_{cp} of light nuclei shows a scaling behavior, which is consistent with a nucleon coalescence mechanism of light nuclei production.

Outlook:

- Working on the compound ratios ($\mathrm{N_p} \times \mathrm{N_t}/\mathrm{N_d^2}$ and $\mathrm{N_p} \times \mathrm{N_{^3He}}/\mathrm{N_d^2}$) in BES-II.
- Continue the analysis of other BES-II (collider + FXT) energies.
- Working on the production of $^{4}\mathrm{He}$ in BES-II.

Thank you for your attention!

Backup

Au+Au collisions at RHIC (Collider mode)				Au+Au collisions at RHIC (Fixed-Target)				
$\sqrt{s_{NN}}$ (GeV)	nEvents (M)	μ_B (MeV)	Time	$\sqrt{s_{NN}}$ (GeV)	E_{beam} (GeV)	nEvents (M)	μ_B (MeV)	Time
200	380	25	Run-10, 19	**13.7**	100	50	280	Run-21
62.4	46	75	Run-10	**11.5**	70	50	320	Run-21
54.4	1200	85	Run-17	**9.2**	44.5	50	370	Run-21
39	86	112	Run-10	**7.7**	31.2	260	420	Run-18, 19, 20
27	585	156	Run-11, 18	**7.2**	26.5	470	440	Run-18, 20
19.6	595	206	Run-11, 19	**6.2**	19.5	120	490	Run-20
17.3	256	230	Run-21	**5.2**	13.5	100	540	Run-20
14.6	340	262	Run-14, 19	**4.5**	9.8	110	590	Run-20
11.5	235	316	Run-10, 20	**3.9**	7.3	120	633	Run-20
9.2	160	372	Run-20	**3.5**	5.75	120	670	Run-20
7.7	104	420	Run-10, 21	**3.2**	4.59	200	699	Run-19
				3.0	3.85	2300	750	Run-18, 21

- STAR has completed BES-II data-taking with factors of 10-20 more statistics compared to BES-I.
- BES-II: 8 collider energies (7.7 – 54 GeV) / 12 FXT energies (3.0 - 13.7 GeV)
- μ_B coverage : $25 < \mu_B < 750$ MeV.

STAR, arXiv:1007.2613
https://drupal.star.bnl.gov/STAR/starnotes/public/sn0493
https://drupal.star.bnl.gov/STAR/starnotes/public/sn0598